

Characterization of FeAl by Powder Metallurgy Route

Huy TD^{1*}, Mohd Sharif N² and Ishihara KN³

¹School of Materials Science and Technology, Hanoi University of Science and Technology, Vietnam

²School of Materials and Mineral Resources Engineering, University of Sains Malaysia, Malaysia

³Graduate School of Energy Science, Kyoto University, Japan

Abstract

Iron aluminum alloy with composition of 30, 35 and 40 at % Al were prepared via powder metallurgy route: mechanical milling, consolidating, sintering. Solid solution Fe (Al) formed after several hours milling, and completely at around 10h from elemental powders. During sintering, phase transformation take place from solid solution Fe(Al) into intermetallic FeAl and carbon impurities from elemental powder lead to an *in situ* precipitation of κ -AlFe₃C_{0.5} simultaneously. Mechanical properties were improving with higher Fe contents and higher sintering temperature with maximum hardness of 5.5 GPa and maximum yield stress of compression test of 700 MPa in the sample of 30 at %Al, 1 h sintering of 1300°C after 10 h milling. The mechanical properties of sintered samples will be discussed in term of microstructure, precipitate and phase formed after sintering.

Keywords: Iron aluminide; Mechanical alloying; Sintering; Precipitate; κ -AlFe₃C_{0.5}

Introduction

Iron and aluminum are common metallic elements used in many industries such as building, automobile or aircraft. Fe-Al alloys are also well-known as advanced materials with many advantageous properties, in particular relatively low cost, low density (as compared with steels), excellent oxidation and corrosion resistance [1-5]. Besides, the Fe-Al alloys are potential candidates for structural application at elevated temperatures and a promising substitute for stainless steels [6] with advantages of their availability as raw materials and as strategic elements for resource conservation (Cr is an example). These advantages have led to the identification of several potential uses including heating elements, heat-exchanger piping, automobile and other industries [7].

In addition, for ages, many researchers have energetically investigated light material with good mechanical properties to save energy resources which are becoming exhausted. Fe-Al alloys are one of candidate for those purposes. Fe-Al alloys are some of candidates for those purposes. However, the Fe-Al alloys show lower mechanical properties than stainless steel. If the mechanical properties of Fe-Al alloys can be improved by employing some sorts of method, they must be applicable in various fields of industries. In general, Fe-Al alloys are strengthened by dispersed hardening method [8-11], where TiC [8], TiN [9] and Fe₃Al with TiB₂ and Al₂O₃ [10,11] are known as the reinforcements, for examples. However, less attention was paid to the strengthening of matrix materials.

Powder metallurgy is well-established method to synthesize a variety of equilibrium and non-equilibrium phases with the structure of nanocrystalline, quasicrystalline, grain refinement or amorphous etc., starting from blended powders [12-14]. Mechanical alloying (MA) such as a ball milling is one of the techniques of powder metallurgy and is a simple and useful processing technique. In MA method, a solid-state reaction proceed involving repeated welding, fracturing and re-welding of powder particles [12,13]. The MA process allows one to overcome problems, such as large difference in melting points of the alloying components as well as unwanted segregation or evaporation that could occur during melting and casting [9]. Thus, the aim of present paper is to investigate the characteristic of Fe-Al alloys formed by MA method. The results are used to understand the mechanical properties and its application to composite materials.

Experimental Procedure

Fe powder of 99.9% purity (300 mesh, Merck) and two different Al powders (100 mesh, 90.0% purity, Merck) and (100 mesh, 99.9% purity, Wako) were used as the starting materials. The composition of Al in the alloy was controlled to be 30, 35 and 40 at %, which are denoted as Fe-30Al, Fe-35Al, and Fe-40Al, respectively. Different mixtures of Al and Fe powders were milled for different milling duration of 0, 2, and 10 h using high-energy planetary ball milling using Pulverisette 5 (Fritsch). The milling process was taken place under argon atmosphere, with the rotation speed of 300 rpm. The vessel with the volume of 500 ml and balls with the diameter of 10 mm which are made from stainless steel, were employed as the milling media. No process control agent (PCA) was used. The ball-to-powder weight ratio was 5:1, and in total about 40 g of samples was used.

The milled samples were compacted under the pressure of 350 MPa using stainless steel die with ϕ 16 mm of inner diameter by means of hydraulic press. The compacted samples were then subjected to sintering process at different temperatures of 1000, 1100, 1200 and 1300°C under low pressure of Ar gas in silica tube. The phase change was investigated by X-ray diffraction (XRD) method using Rigaku RINT2100CMJ with Cu-K α radiation. The microstructure of sample was observed using scanning electron microscopy (SEM, JSM-5800) with energy dispersive X-ray analysis (EDX, EDAX JAPAN). For calculating the average particle size in the milled powder, 10 SEM images have been considered for each sample. About 200 particles from each image have been measured using SI Viewer software. Then the average particle size was calculated using measured particle size from the images.

Mechanical properties of the consolidated compacts were evaluated by Vickers hardness and compression tests. The Vickers hardness was

***Corresponding author:** Huy TD, School of Materials Science and Technology, Hanoi University of Science and Technology, Vietnam, Tel: 84438694242; E-mail: huy.tranduc@mail.hut.edu.vn

Received June 21, 2016; Accepted July 01, 2016; Published July 11, 2016

Citation: Huy TD, Mohd Sharif N, Ishihara KN (2016) Characterization of FeAl by Powder Metallurgy Route. J Material Sci Eng 5: 267. doi:10.4172/2169-0022.1000267

Copyright: © 2016 Huy TD, et al. This is an open-access article distributed under the terms of the Creative Commons Attribution License, which permits unrestricted use, distribution, and reproduction in any medium, provided the original author and source are credited.

measured under the load of 300 g. For the compression test, cubic specimens with the dimension of $2 \times 2 \times 2 \text{ mm}^3$ were prepared from the sintered samples. Errors of approximately $\pm 2\%$ were observed in the Vicker's indentation and compression test. All surfaces of the specimens were polished with 1000 grit SiC paper.

Results

Results of ball milling

When the Al powder (Wako) with higher purity was used for the milling, the sample powders are entirely welded to balls and vessel, and no powdery sample were obtained. On the other hand, in the case of Al powder (Merck) with lower purity, powdery samples were obtained even after 10 hours of milling and the yield of the samples was about 92-95%. After 30 h of milling, the yield was about 20%. In order to investigate the reason for this difference, the natures of impurity in Al powder with lower purity were analyzed. As the result, Al powder with lower purity contained about 2 at % of carbon which may play a role of PCA and contribute to prevent samples from clumping. Hereafter, we will mainly report the results using the Al powder with lower purity. In case of high purity Al (99.9%), it will be denoted as "high purity Al".

Microstructure of milled powder

Figure 1 shows the SEM images of Fe-35Al sample after the milling. The particle size of the sample powder decreases with increasing milling time. After 10 h milling, the milled sample seem to be homogeneous and the average particle size was about $2 \mu\text{m}$. Besides, Fe element cannot be distinguished from Al by mean of EDX analysis.

The XRD profiles of the powders for various milling time are shown in Figure 2. After 1 h of milling, sharp peaks of elemental iron and aluminum can be seen, indicating that both elements remained in the milled mixture. There seem to be no peak of contaminant carbon originated from initial Al powder with lower purity. However, it should be noted that the 0.6 at % of carbon was detected in the milled mixture by mean of the Carbon/Sulfur Determinator (EMIA-520, Horiba). After 10 h of milling, the peaks of Al seem to be almost disappeared. With increasing the milling time, all the remaining peaks with bcc structure shift to lower angle and broaden, and the intensities of all the peaks are weakened. The similar tendency was observed for all the compositions.

Microstructure of sintered sample

Figures 3, 4 and 5 show the XRD patterns for the sample powders of Fe-30Al, Fe-35Al and Fe-40Al milled for 10 h, respectively. The patterns clearly indicated that the sintered samples using Al powder with lower purity consist of intermetallic FeAl with bcc structure accompanied by a small amount of $\kappa\text{-AlFe}_3\text{C}_{0.5}$ carbide phase, while the sintered samples using Al with higher purity consist of only FeAl. For all the compositions, the amount of $\kappa\text{-AlFe}_3\text{C}_{0.5}$ phase shows the largest value

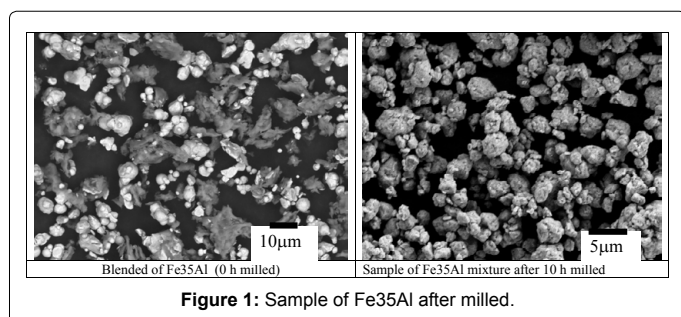


Figure 1: Sample of Fe35Al after milled.

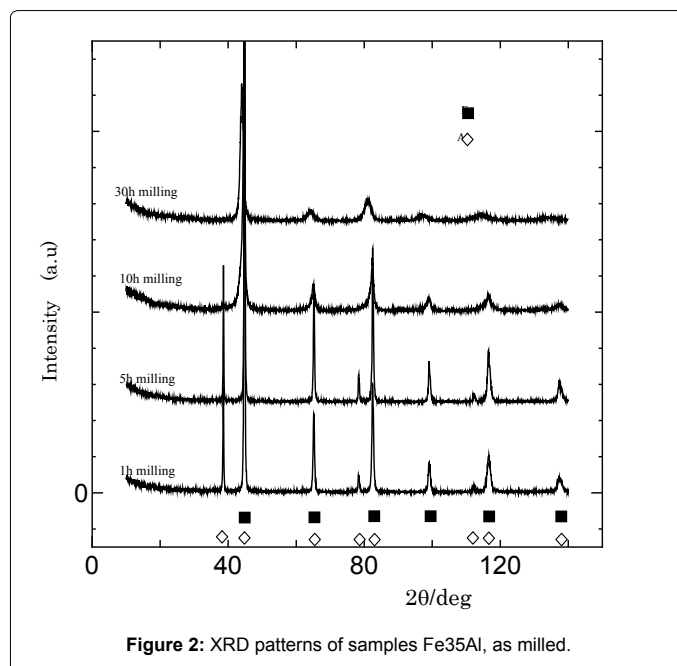


Figure 2: XRD patterns of samples Fe35Al, as milled.

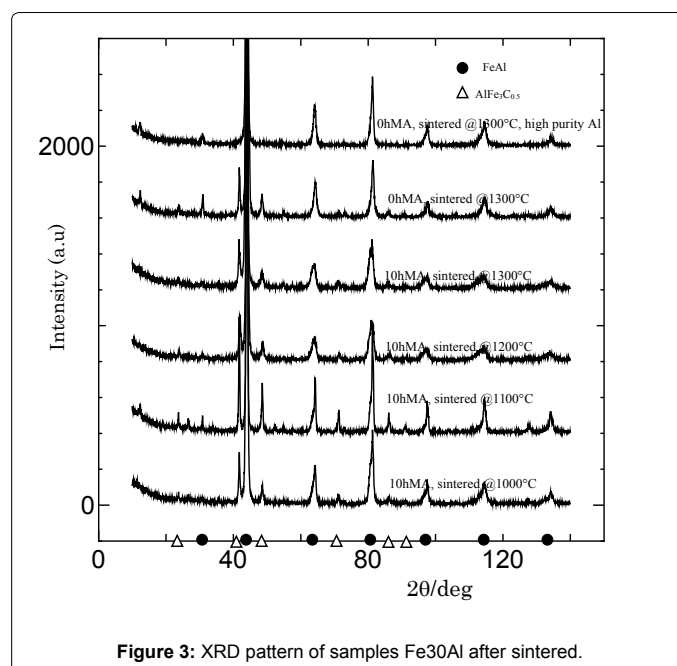
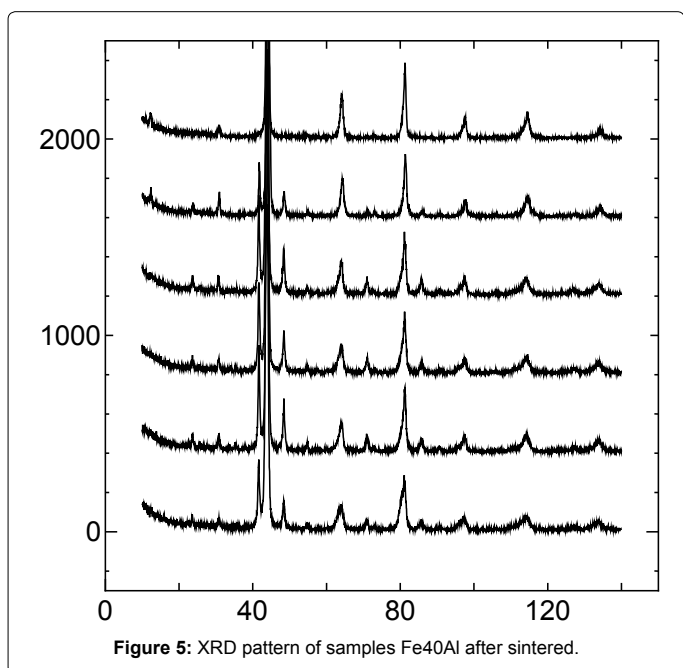
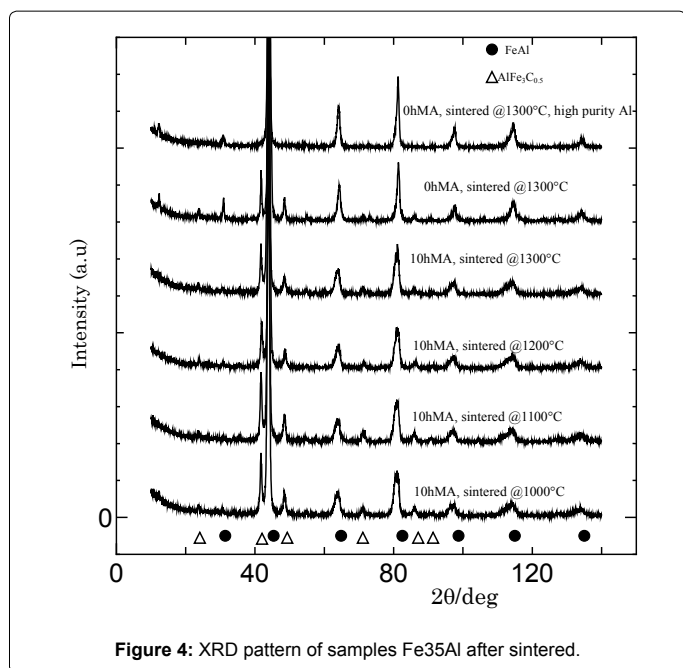


Figure 3: XRD pattern of samples Fe30Al after sintered.

at the sintering temperature of 1100°C . Relative peak of $\kappa\text{-AlFe}_3\text{C}_{0.5}$ precipitated in XRD pattern showed the clear trend under different sintered conditions, as shown in Figure 6.

The lattice parameter (a_0) was measured to confirm the formation of solid solution after milling and intermetallic compound after sintering [15], as shown in Table 1. The lattice parameters of the sintered samples are plotted in Figure 7 as a function of sintering temperature. In the case of Fe-35Al and Fe-40Al, their lattice parameters showed the similar values but are greater than Fe-30Al. It indicates that during sintering, the solid solution transformed to intermetallic compound, which cause the reduction in lattice parameter. Krasnowski et al. [9] showed the result when milling of 45 at.% Fe, 45 at.% Al, 5 at.% Ti and 5 at.% C



after 35 h MA, solid solution Fe(Al) formed with lattice parameter of 2.921 Å.

The contribution of κ -AlFe₃C_{0.5} carbide phase in Fe-35Al alloy showed in Figure 8. It is found that finely dispersed κ -AlFe₃C_{0.5} carbide phase can be seen. The EDAX analysis showed the composition of each element in the κ -AlFe₃C_{0.5} carbide phase, which confirmed the its formation as shown in Figure 9.

Mechanical properties

The results of Vickers hardness test of the sintered Fe-35Al compact are shown in Figure 10. For the comparison, the results for Fe-35Al using high purity Al without MA, which did not include the carbide

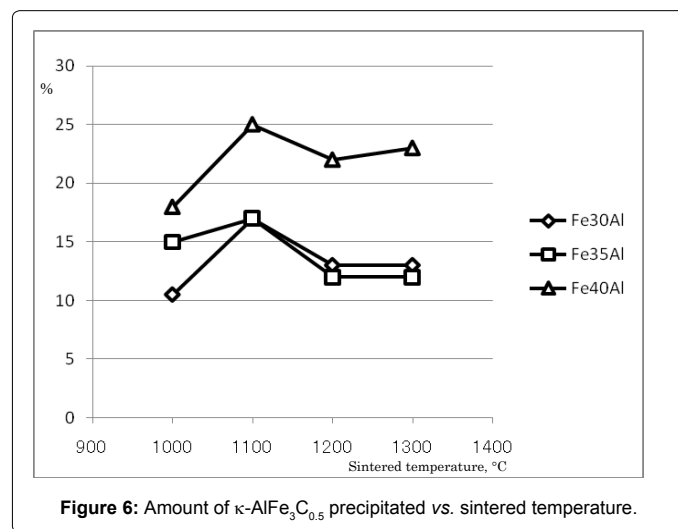
phase, is also shown. It is found that the Vickers hardness of the sample increases with increasing the milling time or sintered temperature. It is also found by comparing the results of the sample using high purity Al with the sample using low purity one that the κ -AlFe₃C_{0.5} phase does not contribute to the hardness. Figure 11 shows the Vickers hardness as a function of sintered temperature for the sample milled for 10 h. The lower the content of Al become, the higher the Vickers hardness becomes, while the effect of sintering temperature seemed to be more significant. As long as our experimental conditions, the maximum hardness, 5.5 GPa was achieved for Fe-30Al at the sintered temperature of 1300°C.

The results of the compression tests for the samples sintered at 1300°C for 1 h with the rate of 0.2 mm/sec are shown in Figure 12. The maximum yield stresses of Fe-30Al, Fe-35Al and Fe-40Al were 720, 690 and 630 MPa, respectively.

Discussion

Factors of mechanical properties

Using Scherrer equation, the crystallite size of Fe-35Al was calculated to be 5.26 nm, after 10 h of milling. After the sintering process, it was increased up to 6.40 nm and 8.1nm at temperature 1000°C and 1300°C, respectively, indicating the coarsening effect. According to Hall-Petch equation, mechanical properties, i.e., strength and hardness will decrease with the increase of crystallite size [7]. However, the mechanical properties of the alloy showed the better results at higher sintering temperature. This suggests us to look at density values, as shown in Table 2. It is found that, at higher sintered temperature, the higher density was obtained. However, the density of sintered samples is relatively low (~83% of theoretical density). Thus



Sample	Lattice parameter as calculated (Å)
Fe elemental powder	2.895
Fe30Al as milled	2.912
Fe30Al sintered at 1300 degree	2.895
Fe35Al solid solution Fe(Al)	2.922
Fe35Al intermetallic FeAl	2.898
Fe40Al solid solution Fe(Al)	2.93
Fe40Al intermetallic FeAl	2.898
Fe50Al as milled (Krasnowski et al. [9])	2.921

Table 1: Calculated lattice parameter of samples.

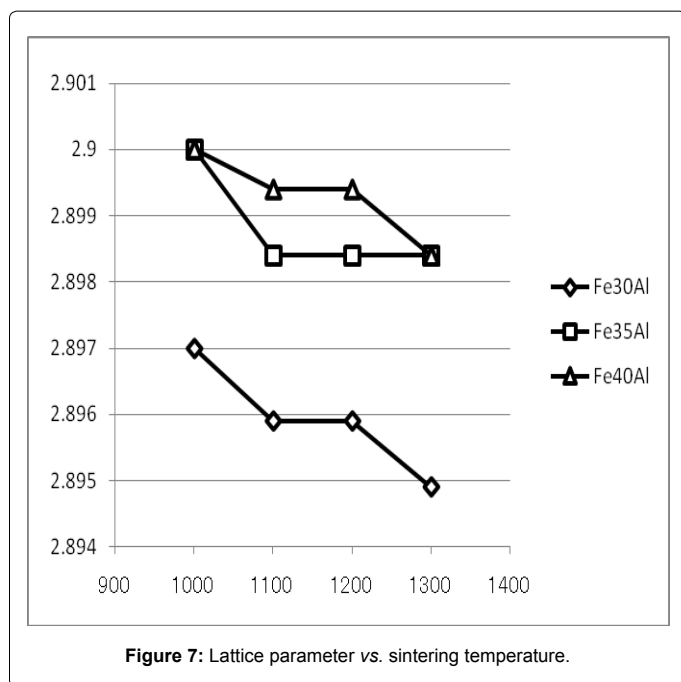


Figure 7: Lattice parameter vs. sintering temperature.

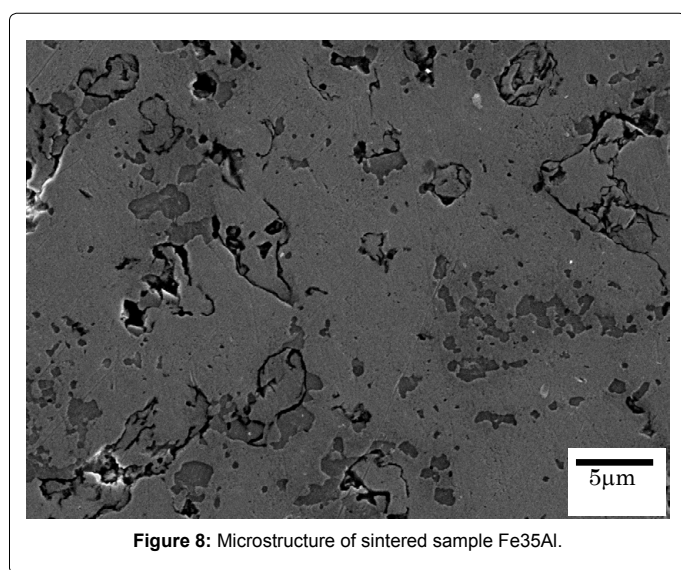


Figure 8: Microstructure of sintered sample Fe35Al.

the density of sintered samples strongly affected on the mechanical properties. As the results, the decrease of mechanical properties due to the increase of crystalline size was compensated by the increase of density which led to the increase of mechanical properties.

As for the effect of MA on the mechanical properties, it is well-known that MA brings about considerable lattice defects such as dislocation. In case of Fe-Al system, it was reported that point defect in B2 site of FeAl are introduced, which is anti-site Al atom, anti-site Fe atom, vacancy on β (Al) sublattice and vacancy on α (Fe) sublattice [7,16,17]. Since the lattice defects contribute to the increase in some sort of mechanical properties, the Vickers hardness and yield stress of the sample with increasing milling time.

Finally, we will focus on the existence of carbide phase, κ -AlFe₃C_{0.5}. It originally comes from the stabilizer of Al powders, but seems to play a role as PCA as mention above. The sample including the carbide phase

showed the almost same hardness value as the sample without carbide phase using high purity Al. It suggests that the strength of carbide phase is similar to that of intermetallic FeAl. It might be applicable to the mechanical alloying, since we can use the stabilized, popular aluminum powders as starting materials instead of the high purity reagents. In addition, the amount of carbide phase is changed depending on the sintering temperature as shown in Figure 6 [18-20]. The maximum of carbide phase when sintered at 1100°C, but at higher sintering temperature, its amount decreases and seems to be stable at sintering temperature of 1200 and 1300°C. This may due to the loss of carbon at high sintering temperature. Thermodynamically, it suggests that Al₄C₃ may be formed from κ -AlFe₃C_{0.5} carbide phase [21,22]. The formation of Al₄C₃ caused the reduction of total κ -AlFe₃C_{0.5} phase.

As mentioned before, the high purity aluminum cannot mill even an hour. Therefore, we only can compare the effect of κ -AlFe₃C_{0.5} carbide phase in the case of no milling. The results show a small different, which is the FeAl alloy with presence of κ -AlFe₃C_{0.5} carbide phase possess a bit higher hardness. The lower purity aluminum can mill for long time, even up to 30 h. In this case, carbon impurity play a role as PCA and then, κ -AlFe₃C_{0.5} carbide phase formed after sintering. The milling process also reduced grain size of carbon, and κ -AlFe₃C_{0.5} carbide phase precipitated during sintering was very fine distribution in FeAl alloy. This is also important to mechanical properties. The fine particulate of κ -AlFe₃C_{0.5} carbide will strengthen the FeAl alloy by impeding the motion of dislocation [4,13]. The alloy remains the major load bearing constituent and will be strengthened in proportion to the effectiveness of the dispersion as a barrier to dislocation movement.

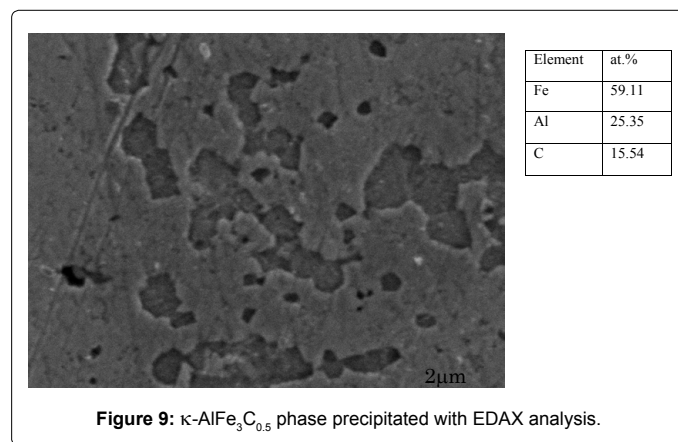


Figure 9: κ -AlFe₃C_{0.5} phase precipitated with EDAX analysis.

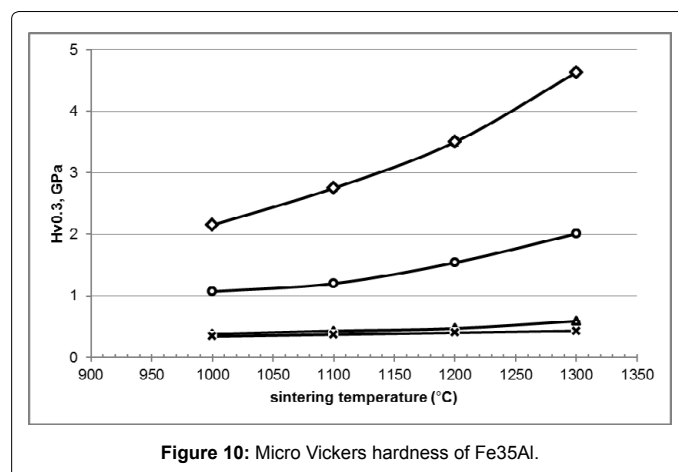


Figure 10: Micro Vickers hardness of Fe35Al.

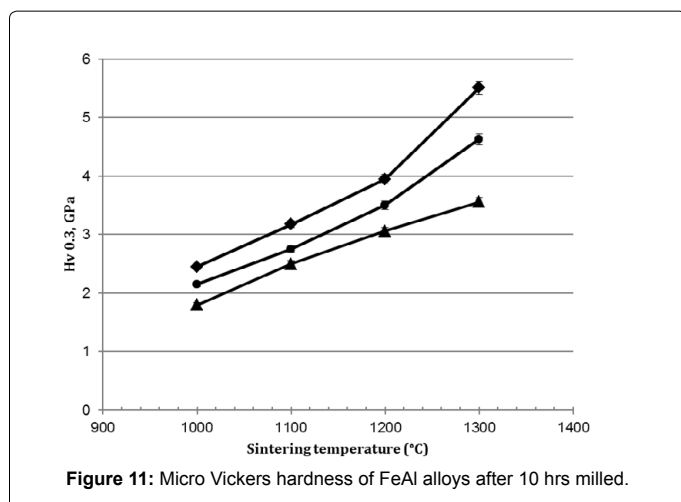


Figure 11: Micro Vickers hardness of FeAl alloys after 10 hrs milled.

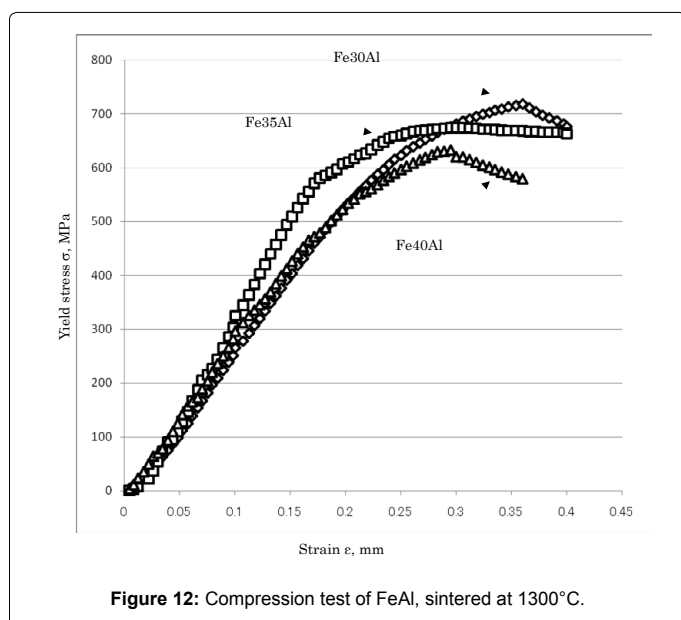


Figure 12: Compression test of FeAl, sintered at 1300°C.

Sample	Density (g/cm ³)
Fe35Al 0 h milling, high purity Al, sintered at 1300°C	4.995
Fe35Al 0 h milling, sintered at 1300°C	4.963
Fe35Al 10 h milling, sintered at 1300°C	5.316
Fe35Al 1 h milling, sintered at 1300°C	5.124
Fe35Al 10 h milling, sintered at 1100°C	5.207
Fe35Al 1 h milling, sintered at 1100°C	5.029
Fe35Al ideality, calculated	6.015

Table 2: Density of samples Fe35Al.

Comparison with literatures

Moris et al. [18,19] reported that the Vickers hardness of the sample with the composition of Fe-40Al consolidated by hot isostatic pressing (HIP) after 10 h of ball milling with 1 at.% of Y₂O₃ was 3.5 GPa, which is similar to our results as shown in Figure 11. Another result of Fe-28Al using Tubular shaker for 24 h and subsequent spark plasma sintering by Zadra et al. [16] showed the hardness of 5.2 GPa, which is slightly lower than our results, 5.5 GPa (Figure 11). The reason for these differences would be due to the nature of each mechanical alloying method. The

ball milling and shaker may be need much longer time to get the improved in mechanical properties. The planetary ball milling is high energy process because of high rotating speed, which caused to large amount of defects.

L. Pang et al. [5] reported the yield streng of 512 MPa for Fe-40Al formed by induction melting method, which is lower than our results, 630 MPa. This showed the advantageous of milling process to the mechanical properties. By using milling, the grain size was significant decreased, which improve the strength due to Hall-Petch equation.

The results of hardness and compressive strength showed the properties of FeAl intermetallic compound with presence of κ-AlFe₃C_{0.5} carbide phase. The improvement mechanical properties by reinforcement phase promising many interesting. Further work is need to applied this result to fabricate FeAl base composite with multi reinforcements such as TiB₂, TiC and Al₂O₃ is very attractive to understand how they affect each other.

Conclusion

The results of this work showed that Solid solution Fe(Al) formed after 10 hours milled for the alloys of Fe-30Al, Fe-35Al and Fe-40Al from elemental powders Fe and Al (product of Merck Co. Ltd.) After sintering, phase transformation from solid solution Fe(Al) into intermetallic FeAl. *In situ* precipitated of κ-AlFe₃C_{0.5} carbide phase after sintering process and this phase not effect to mechanical properties of sample. The sintering temperature at 1300°C in 1 hour showed the best results in mechanical properties. Mechanical properties of FeAl alloys were improved by mechanical alloying.

Acknowledgement

This work was supported by The Japan International Cooperation Agency (JICA) under the Asia University Network/Southeast Asia Engineering Education Development Network (AUN-SEED/Net) Program. Thanks are also due to the School of Materials and Mineral Resources Engineering, Universiti Sains Malaysia, Malaysia and Graduate School of Energy Science, Kyoto University, Japan for the facilities provided.

References

- Suryanarayana C (2001) Mechanical alloying and milling. Progress in Materials Science 46: 1-184.
- Zhu SM, Tamura M, Sakamoto K, Iwasaki K (2000) Characterization of Fe₃Al-based intermetallic alloys fabricated by mechanical alloying and HIP consolidation. Materials Science and Engineering A 292: 83-89.
- Park BG, Ko SH, Park YH, Lee JH (2006) Mechanical properties of in situ Fe3Al matrix composites fabricated by MA-PDS process. Journal of Intermetallic 14: 660-665.
- Krasnowski M, Grabias A, Kulic T (2006) Phase transformations during mechanical alloying of Fe-50% Al and subsequent heating of the milling product. Journal of Alloys and Compounds 424: 119-127.
- Pang L, Kumar KS (1998) Mechanical behavior of an Fe-40Al-0.6C alloy. Acta Mater 46: 4017-4028.
- Moris DG, Munos-Moris MA, Chao J (2004) Processing and Applications of Intermetallic γ-TiAl-Based Alloys. Journal of Intermetallic 12: 821-826.
- Varin RA, Bystrzycki J, Calka A (1999) Effect of annealing on the microstructure, ordering and microhardness of ball milled cubic (L1₂) titanium trialuminide intermetallic powder. Journal of Intermetallic 7: 785-796.
- Moris DG, Munos-Moris MA, Baudin C (2004) The high-temperature strength of some Fe₃Al alloys. Acta Materialia 52: 2827-2836.
- Krasnowski M, Witek A, Kulic T (2002) The FeAl-30%TiC nanocomposite produced by mechanical alloying and hot-pressing consolidation. Journal of Intermetallics 10: 371-376.

10. Kang HZ, Lee S, Hu CT (2005) The role of pre-formed Fe₂Al₅ in P/M processing of Fe₃Al. *Materials Science and Engineering A* 398: 360-366.
11. Sebastian V, Lakshmi N, Venugopalan K (2007) Structural and properties of mechanically alloyed Fe-66at%Al. *Journal of Intermetallic* 15: 1006-1012.
12. Sebastian V, Lakshmi N, Venugopalan K (2007) Correlation between microstructure and magnetic properties in mechanically alloyed nanogranular Fe_{100-x}Al_x. *Journal of Materials Letters* 61: 4635-4368.
13. Krein R, Schneider A, Sauthoff G, Frommeyer G (2007) Microstructure and mechanical properties of Fe₃Al-based alloys with strengthening boride precipitates. *Journal of Intermetallic* 15: 1172-1182.
14. Stoloff NS (1998) Iron aluminides: present status and future prospects. *Materials Science and Engineering A* 258: 1-14.
15. Lihn VF, Jarhgang HE (1961) An implicit time-integration procedure for a set of internal variable constitutive equations for isotropic elasto-viscoplasticity. *International journal of plasticity* 32: 483-487.
16. Zadra M, Casari F, Lonardelli I, Ischia G, Molinari A (2007) In-situ precipitation of Al₂O₃ and κ-Fe₃AlC_{0.5} in iron aluminides through spark plasma sintering: Microstructures and mechanical properties. *Journal of Intermetallic* 15: 1650-1658.
17. Munos-Moris MA, Garcia Oca C, Morris DG (2003) Microstructure and room temperature strength of Fe-40Al containing nanocrystalline oxide particles. *Acta Materialia* 51: 5187-5197.
18. Morris DG, Gutierrez-Urrutia I, Munos-Morris MA (2008) Ratcheting in cyclic plasticity II: Multiaxial behavior. *International Journal of Plasticity* 24: 1205-1223.
19. Morris DG, Munos Morris MA, Requejo LM (2006) New iron-aluminium alloy with thermally stable coherent intermetallic nanoprecipitates for enhanced high-temperature creep strength. *Acta Materialia* 54: 2335-2341.
20. Yang HT, Li CJ, Yang GJ, Li CX (2009) On Gauge Invariance and Vacuum Polarization. *Vacuum* 83: 146-152.
21. Connetable D, Lacaze J, Maugis P, Sundman B (2008) Phase field simulations in miscibility gaps. *Computer Coupling of Phase Diagrams and Thermochemistry* 32: 361-370.
22. Ohtani H, Yamano M, Hasebe M (2004) Thermodynamic analysis of the Fe-Al-C ternary system by incorporating ab initio energetic calculations into the CALPHAD approach. *ISIJ International* 44: 1738-1747.